Catalysis Letters
https://doi.org/10.1007/s10562-020-03394-7

Perspective on Catalytic Biomass Pyrolysis Bio-oils: Essential Role of Synergistic Effect of Metal Species Co-substitution in Perovskite Type Catalyst

Rahmiye Zerrin Yarbay Şahin[1,2] · **Nurgül Özbay**[1]

Received: 24 July 2020 / Accepted: 14 September 2020

Abstract

Due to being an economic alternative to various oxides and even noble metals in many catalytic applications, perovskites are getting interest day by day by the researchers. The aim of this study is to evaluate the synergistic effect of metal species co-substitution in perovskite type catalysts in different biomass types pyrolysis process. Thus, evaluating the feedstocks and pyrolysis products in terms of yields, quality and potential use is successfully achieved. Perovskite-type catalysts $LaCo_{0.5}Mn_{0.5}O_3$, $LaMn_{0.5}Ni_{0.5}O_3$ and $LaCo_{0.5}Ni_{0.5}O_3$ were prepared by sol–gel method, characterized by N_2 adsorption–desorption, XRD and SEM techniques, and performed in the catalytic pyrolysis of two biomass samples (date seed and mandarin peel) in a tubular reactor at 520 °C with 100 °C/min and 100 cm^3/min N_2 atmosphere. Partial substitution of B′ was found to favor the catalytic activity as compared to non-catalytic results. The best pyrolysis performance was obtained with $LaMn_{0.5}Ni_{0.5}O_3$, achieving maximum bio-oil yield of 28.33 and 25.73% for date seed and mandarin peel, respectively. Moreover, the best performance of $LaMn_{0.5}Ni_{0.5}O_3$ signifies the best synergistic effect between Ni and Mn. The bio-oil characterization including elemental analysis, ^{1}H-NMR, FT-IR, and GC–MS results showed that catalysts favored to increase the H content and decrease the O content. It was also established that the bio-oil produced from date seed has the highest potential respecting upgrading the bio-oil to achieve valuable chemicals.

Graphic Abstract

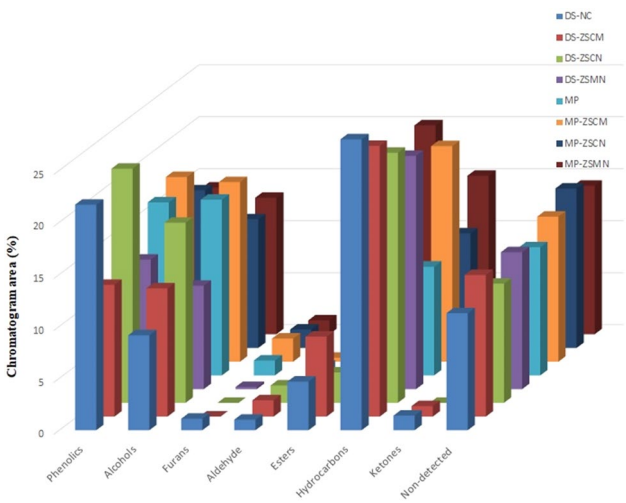

Electronic supplementary material The online version of this article (https://doi.org/10.1007/s10562-020-03394-7) contains supplementary material, which is available to authorized users.

Extended author information available on the last page of the article

Published online: 23 September 2020

Keywords Catalytic pyrolysis · Date seed · Mandarin peel · Perovskite · Synergistic effect

Abbreviations

DS	Date seed
MP	Mandarin peel
ZSMN	$LaMn_{0.5}Ni_{0.5}O_3$
ZSCM	$LaCo_{0.5}Mn_{0.5}O_3$
ZSCN	$LaCo_{0.5}Ni_{0.5}O_3$
NIST	National Institute of Standards and Technology
FTIR	Fourier-transform infrared spectroscopy
GC–MS	Gas chromatography–mass spectrometry
HHV	Higher heating value
HC	Hydrocarbon

1 Introduction

Biomass is known as one of the common renewable energy sources in the light of energy use [1]. In order to evaluate the agronomic benefits of biomass, several factors as well as the biomass feedstock selection and transportation requirements should be taken account. Although, the process seems far away from commercialization, investigations at lab scale are the most important cooperators to show the way to build up more efficient production processes and novel alternative or added-value uses for biomass species. Pyrolysis is a promising answer in the field of biomass processing into energy-valuable fuels in terms of high-calorie gaseous, liquid and solid [1]. The biomass is generally reliant to location of interest for the pyrolysis production [2] and possible biomasses comprise wastes from the forest and agriculture and grass in Turkey. According to Oasmaa et al. agro-based biomasses are challenging because of the high amount of alkali metals and nitrogen in the feedstocks [3].

The catalytic pyrolysis of biomass is an effective methodology not only to recover the bio-oil quality but also to develop selectivity to desired chemicals. Due to biomass` complex nature, different additives/catalysts to optimize the pyrolysis are expected to face with [4]. The catalytic pyrolysis can be realized either in-situ or ex-situ. In in-situ pyrolysis, pyrolysis vapors approach to the catalyst surface thus making possible to cracking, deoxygenation and converting to more desired chemicals like as aromatic hydrocarbons and phenols [5]. Selecting the suitable catalyst for pyrolysis is still under investigation with the aim of achieving high quality bio-oil with low oxygen content besides converting the undesired chemicals into desired ones in the pyrolysis vapors while displaying thermal stability therewithal long lifetime [6, 7].

In recent times, perovskite-type oxides (with ABO_3 formula) are studied in many applications like sensors, electrochemistry, solar cell, and catalysis [8]. Perovskites are known with their superior structure with a ReO_3-type framework made up by incorporation of A cations into BO_6 octahedron. In octahedron structure, A site is generally selected as an alkaline-earth, alkali or other larger ions and the B site was made of many transition metal cations with relatively smaller radius. This octahedron structure allows the perovskites to carry on changes in their A and/or B sites by partially substituting other metal ions [9]. This situation could persuade structural distortions and/or B site valence transformations thus changing their physiochemical properties for desired application [8, 9]. On the other hand, substitution of metals into A and/or B sites could recover the reactivity of the perovskites [10–13]. For that reason, perovskites with doped of metals in A or B sites were more and more searched to lay out [8, 9, 14]. According to the literature, the best catalysts are found as compounds containing transition metal Mn, Fe, Co or Ni in the B-site for complete oxidation, and the outcome of a partial substitution of the cation B by B′ of similar oxidation state and ionic radius can improve perovskite stability or enhance their redox performances. The synthesis of bimetallic catalysts through partial substitution reduces catalyst costs like Co and generates new active sides [10]. Cihlar [11] studied the catalytic behavior of the prepared perovskite oxides of $La_xCa_{1-x}M_yAl_{1-y}O_{3-d}$ (M = Co, Cr, Fe, Mn; x = 0.5; y = 0.7–1.0) for methane oxidation. The oxidation performance was decided by the active centers formed by transition metal ions and oxygen vacancies thus La–Ca–Co–Al–O had higher methane conversion and hydrogen selectivity. Santos et al. [12] developed $LaNi_{1-x}Co_xO_3$ (x = 0.0, 0.2, 0.5 and 1.0) for partial oxidation of methane and results showed that H_2 pretreatment of perovskite was beneficial for the generating of active species, and subsequently favored the partial oxidation of methane. The partially reduced Co on the surface was found to be beneficial to the resistance to carbon formation. Zhang et al. showed that substitution of Mn by Fe can be interesting due to the Fe^{3+} and Mn^{3+} ions present the same size; therefore, dramatic structural changes would not expect. Based on this, doping of Mn^{3+} ions to Fe site may just cause the distortion of the crystal structure [15].

According to these studies, it is concluded that the different metals in perovskite oxides take part in different roles for the activity. Although the metal in A-site is well known as being non-catalytic. It exhibits an indirect effect on reactivity throughout altering the amounts of oxygen vacancies and the valence states of B-site elements [8]. Therefore, more and more effective perovskites are found to worth to investigate.

Despite studying the metal doped in A or B site in many catalytic applications, none of the studies was related to biomass pyrolysis. The aim of this study, (i) synthesize

perovskite catalysts, (ii) use in two different biomass' pyrolysis and (iii) figure out the synergistic effect of metal species co-substitution in pyrolysis yields and pyrolysis bio-oil content. Thus, this study aims to fill the lack of this area related to current subject. According to this, $LaBO_3$ catalysts were prepared by sol–gel method. The influences of the substitution were explored in terms of physicochemical properties and catalytic performances of biomass pyrolysis.

2 Materials and Methods

2.1 Biomass

The air-dried date seed and mandarin peel was sieved and the average particle size for the biomass samples was found as 1.026 mm and 0.882 mm, respectively. The bulk densities of biomass' were determined as 0.56 g/cm^3 and 0.26 g/cm^3 for date seed and mandarin peel according to ASTM 321-D standards, respectively. The ultimate analysis of the biomass samples was evaluated via a Leco CNH628 S628 elemental analyzer. The elemental, ultimate and proximate analyses results can be found in the Table S1 in Supplementary File.

2.2 Catalyst Preparation

$LaB_xB(_{1-x})O_3$ (y = 0–0.5) catalysts were arranged by sol–gel synthesis [16]. The detailed preparation procedure is available in the reference. The catalysts were fired in air at 700 °C for 5 h with 10 °C/min heating rate. The catalysts were denoted as ZSCM, ZSMN and ZSCN for $LaCo_{0.5}Mn_{0.5}O_3$, $LaMn_{0.5}Ni_{0.5}O_3$ and $LaCo_{0.5}Ni_{0.5}O_3$ respectively.

2.3 Experimental Method

The pyrolysis tests were performed in an electrically heated stainless-steel tubular reactor size of 2.5 cm id and 90 cm length. The reactor is externally heated by an electric furnace and the reactor temperature is monitored by a thermocouple inside the bed. Sweeping gas was N_2 with 100 mL/min flow rate in order to preserve the inert atmosphere inside the reactor. The tests were implemented at fixed conditions (temperature: 520 °C; heating rate: 100 °C/min; residence time: 15 min). Although 10 g of biomass was used in non-catalytic pyrolysis tests, 0.5 g catalyst and 9.5 g biomass were used in catalytic runs. The catalyst/biomass ratio was determined according to our previous studies related to catalytic pyrolysis [17].

The pyrolysis products were liquid, solid char and non-condensable gases. The liquid product was first condensed in collecting bottles which preserved at about 0 °C and then recovered by washing with dichloromethane solvent. The liquid was further divided into bottom aqueous (called here as water) phase and top organic phase (called here as bio-oil) via separating funnel. Bio-oil was dried first by using anhydrous sodium sulphate. Afterwards, dichloromethane solvent was evaporated at almost 40 °C and 790 mbar using a rotary evaporator.

It should be noted that the biomass and perovskite catalyst were mixed physically. Thus, it is not possible to separate at the end of pyrolysis experiment. Indeed, during calculations, no mass change in the catalyst was considered. As a consequence, the yield of bio-oil, char and gaseous product was calculated as percentage weight basis follows (Eqs. (1), (2), (3):

$$Bio\text{-}oil\ yield\ (wt\%) = \frac{mass\ of\ bio\text{-}oil}{mass\ of\ biomass} \quad (1)$$

$$Char\ yield\ (wt\%) = \frac{mass\ of\ solid\ product - mass\ of\ catalyst}{mass\ of\ biomass} \quad (2)$$

$$Gaseous\ product\ yield\ (wt\%) = 100 - (Bio\text{-}oil\ yield - Char\ yield) \quad (3)$$

The biomass conversion was evaluated as stated below [18]:

$$Conversion(wt\%) = \frac{(mass\ of\ bio\text{-}oil) + (mass\ of\ gas) + (mass\ of\ water)}{mass\ of\ biomass} * 100$$
$$= 100 - (mass\ of\ char)$$

2.4 Analytical Techniques

The bio-oil characterization was evaluated using elemental analysis, FT-IR, TGA, GC–MS and ^{1}H-NMR. Elemental results (Leco CNH628 S628) were conducted on a dry ash-free basis. A thermogravimetric analyzer (Setaram Labsysevo) was run for monitoring the thermal behavior of the biomass types. Gas chromatography/mass spectroscopy (GC–MS) analysis of bio-oils were achieved via a QP2010 Model gas chromatograph and a mass selective detector (Shimadzu, Japan); a thin film (30 m × 0.25 mm, 0.25 µm film thickness). Teknoroma TRB-5 MS capillary column was utilized. Helium was used as a carrier gas with 1 cm^3/min flow rate. The temperature was set to 40 °C for 5 min followed by 4 °C/min heating rate to 260 °C. The compounds were recognized using NIST library. The FT-IR spectrum was documented using a Perkin Elmer Spectrum 100 Model. ^{1}H-NMR spectra of bio-oils were examined using Agilent 400 MHz Premium Compact, TMS as the internal standard and detorochloroform ($CDCl_3$, Merck) was used as the solvent.

The specific surface area (m^2/g) of the catalysts was checked by N_2 porosimetry (BET) at 77 K using

Micromeritics ASAP 2020 System. Phase identification of the catalysts was done by X-ray diffractometer using Panalytical Empyrean diffractometer at 40 kV under Ni-filtered CuKα radiation (λ = 0.15418 nm). SEM micrographs were obtained in a Zeiss Supra VP 40.

3 Results and Discussion

3.1 Characteristics of Prepared Catalysts

The synergistic effect of metal species co-substitution in crystal structure of the catalysts were investigated via XRD patterns. The XRD spectra of 2Θ = 0°–70° of the perovskite type catalysts investigated for synergistic effect are given in Fig. 1. The orthorhombic $LaCo_{0.5}Mn_{0.5}O_3$ phase (PDF No. 98-016-4463) in the XRD spectrum of the ZSCM, hexagonal $LaCo_{0.5}Ni_{0.5}O_3$ phase (PDF No. 98- in the ZSCN and the orthorhombic $LaMn_{0.5}Ni_{0.5}O_3$ phase (PDF No. 98-016-4966) in the ZSMN were obtained. The desired and perfect pure phases were observed in all compositions.

BET surface areas of catalysts as given in Table 1 were fallen between 7.32 and 9.52 m^2/g. The surface area of the catalysts is found as low as expected which can be also seen from the literature [13, 16]. The values are also close to each other. It can be stated that in presence of cobalt, bigger pore size was achieved. In all compositions, nickel is found to favor to grow the pore size. The adsorption/desorption graphs of the synthesized catalysts obtained under liquid nitrogen are given in Fig. 2. According to the Fig. 3, all catalysts showed type III isotherm and H3-type hysteresis which were defined by IUPAC. Indeed, average pore diameter indicated that the catalysts were macroporous.

The SEM images at ×20 magnification ratios were given in Fig. 4. All the catalysts showed quite porous and spongy structure. In the case of manganese metal, more porous structures were obtained. In terms of ZSMN, bigger holes instead of small holes were observed. ZSMN was found as the most spongy-like structured catalyst among studied samples.

Table 1 Textural properties of the samples synthesized

Sample	S_{BET} (m^2/g)	Vp (cm^3/g)	Dp (nm)
$LaMn_{0.5}Ni_{0.5}O_3$	7.32	0.039	22.68
$LaCo_{0.5}Ni_{0.5}O_3$	8.64	0.043	23.89
$LaCo_{0.5}Mn_{0.5}O_3$	9.52	0.049	22.84

S_{BET} BET surface area, *VP* total pore volume, *DP* pore diameter

3.2 Catalytic Activity

The product yields and conversion of biomass of the non-catalytic and catalytic pyrolysis are given in Fig. 5. The results confirmed that yields changed with biomass type. Results showed that date seed (DS) gave greater liquid yield than mandarin peel (MP). All catalysts have improved the bio-oil yield compared to non-catalytic runs but the highest bio-oil yield is achieved with ZSMN catalyst. This performance can be attributed to the cracking activity of Mn and combined effect of Ni–Mn catalysts. Increment in bio-oil yield for all catalytic runs can be explained with enough residence time of the non-volatiles on the catalyst surface. If released volatiles from biomass stay shorter enough on the catalyst surface, this will result as preventing secondary reactions including dehydrogenation, depolymerization and fragmentation thus increasing the overall liquid yield. While cobalt and nickel containing catalysts resulted bad in terms of liquid yield, further it would seem promote the formation of non-volatile gaseous products. On the other hand,

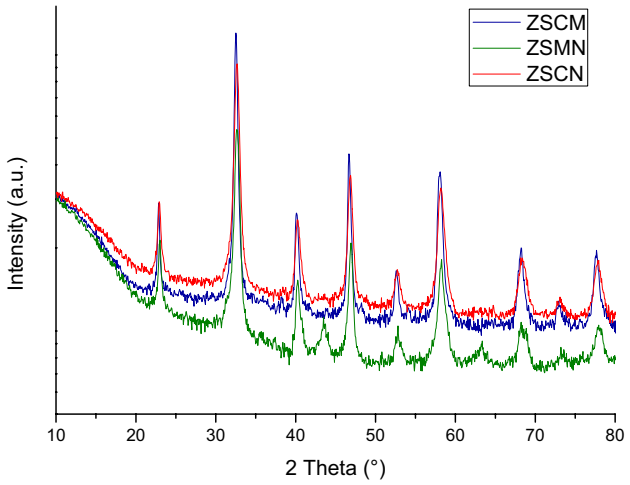

Fig.1 XRD spectrum of the samples

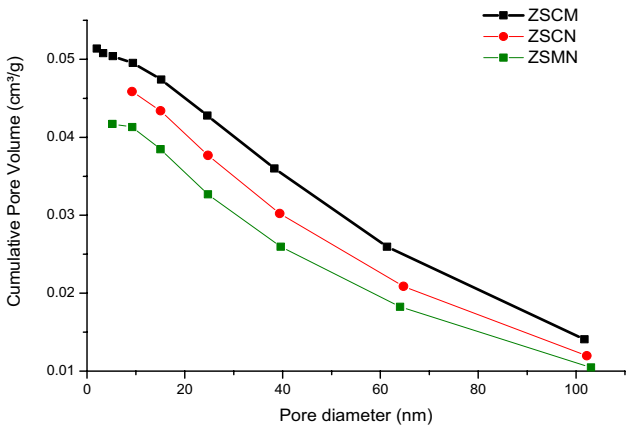

Fig. 2 BJH adsorption cumulative pore volume graphs of the catalysts

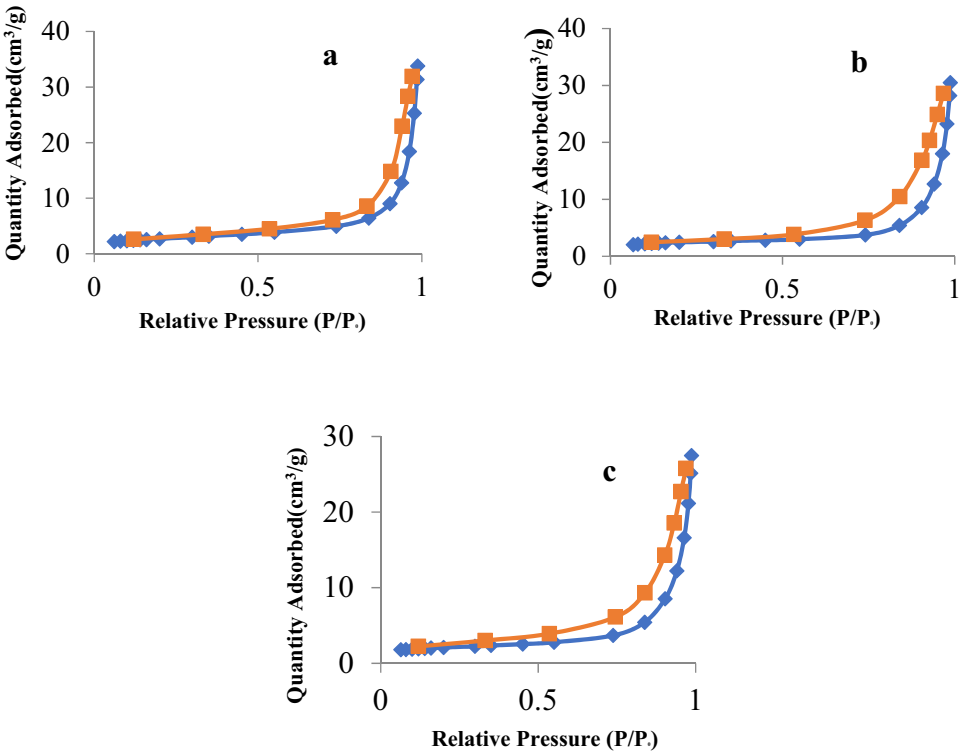

Fig. 3 N_2 adsorption/desorption isotherms of **a** ZSCM, **b** ZSCN, and **c** ZSMN catalysts

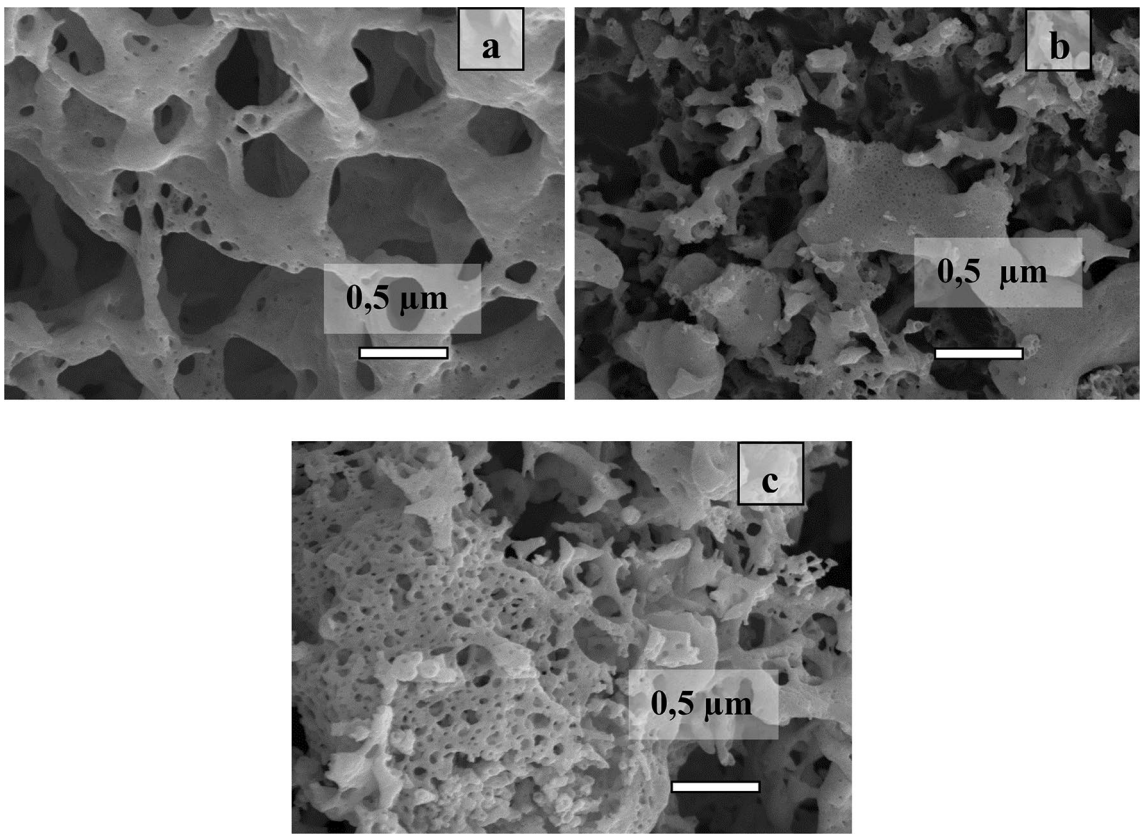

Fig. 4 SEM images of **a** ZSMN, **b** ZSCN and **c** ZSCM

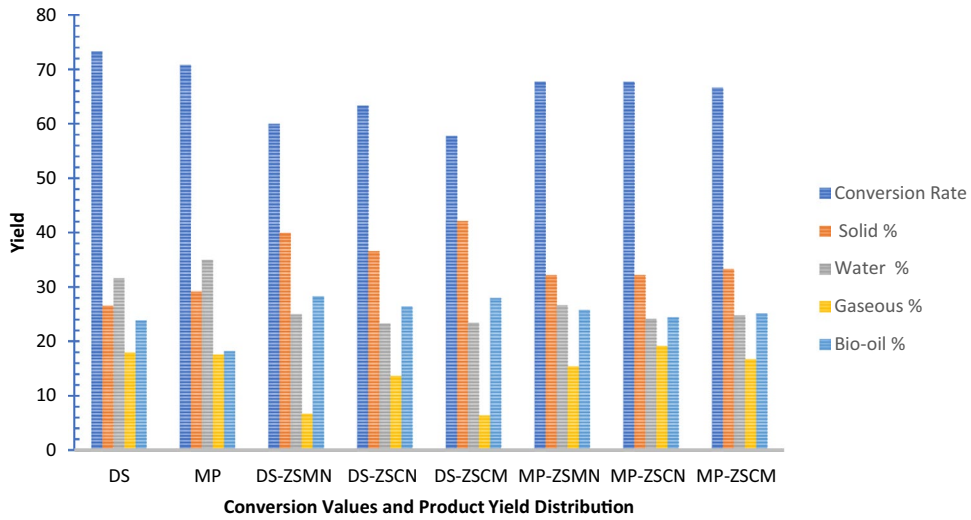

Fig. 5 Products yield distribution of thermal and catalytic experiments

the increased solid product yields which was observed for all catalytic runs were due to the formation of coke on the surface of the catalyst. Besides, since DS with higher lignin content gave higher char yields in catalytic runs when compared with more cellulosic MP. Although non-catalytic char result of DS was expected greater than MP due to higher lignin content, char yields of both biomasses was found to similar to each other. It can be stated that the catalysts also favored decomposition of lignin and showed selectivity to decomposition of this biomass component. The non-condensable gas yields were reduced with presence of catalysts because of the formation of more condensable vapors.

Although the catalytic bio-oil yields of mandarin peel were low, the conversions of mandarin peel were found to be high. This could be clarified by the holocellulose content. This content was higher than date seed, whereas the decomposition of holocellulose favored the formation of water-soluble HCs rather than oily chemicals (water insoluble) causing low bio-oil yield which situation is also observed for other biomass species in the literature [19].

The performance of a catalyst except conversion changes with different factors which are more depend on reactions besides reactants used. Working with catalytic materials could lead the formation of desired products like hydrocarbons, furans, phenols, etc. while promoting reactions such as dehydration, decarboxylation, decarbonylation, dehydrogenation and cracking [20]. According to this, the effectiveness ($K_{effectiveness}$) plays a vital role to figure about the performance of the catalyst [21]. This value can be calculated by multiply the yield (Y) and selectivity (S). It is possible to calculate Y as dividing the weight of the desired product to the weight of the biomass as dry ash. S can be achieved from the proportion of desired product (wt%) to undesired product (wt%).

The effectiveness of the catalysts is given in Fig. 6. Among the synthesized perovskites the effective catalyst was ZSMN for both biomass samples. The ZSMN catalyst was followed by the ZSCM and ZSCN catalysts, respectively. Manganese was the most active metal among the used ones. Nickel was the second active metal. Although the perovskites effected the mandarin peel conversion intensively, the effectiveness seemed lower than date seed when effectiveness values compared.

The performance of the Co, Mn and Ni containing perovskite catalysts for date seed pyrolysis were evaluated by Özbay and Yarbay Şahin [22]. The effectiveness of Co, Mn and Ni was found as 6.02, 7.18 and 7.10, respectively. When compared the synergistic catalyst with B` site undoped catalysts, the second metal substitution approved the positive synergistic effects between Ni, Co and Mn ions. This progressive effect was thought to be initiated by the enhanced activities, reduced band-gap energies and increased local density of states values across the Fermi level. As taking account the ZSMN, the synergistic effect of Mn and Ni species expands the dispersion of NiO_x and MnO_x species by improving the interaction between the loaded metal oxides and biomass; it also makes stronger the interaction between the NiOx and MnOx species. The brought Ni–O–Mn mixed bonds and following rise in lattice defects favor the generation of surface-adsorbed oxygen species with high mobility to quicken biomass decomposition.

The low H/C ratio of biomass is accepted to be responsible for fast deactivation of catalysts in pyrolysis. Indeed, this low ratio withdraws a low amount of hydrogen in the hydrocarbon pool inside catalyst through pyrolysis of biomass. This phenomenon is known to effect an improved polymerization degree of coke-maker molecules. Coke formation inside the catalyst structure drops the catalyst activity and consequently the efficiency of the pyrolysis

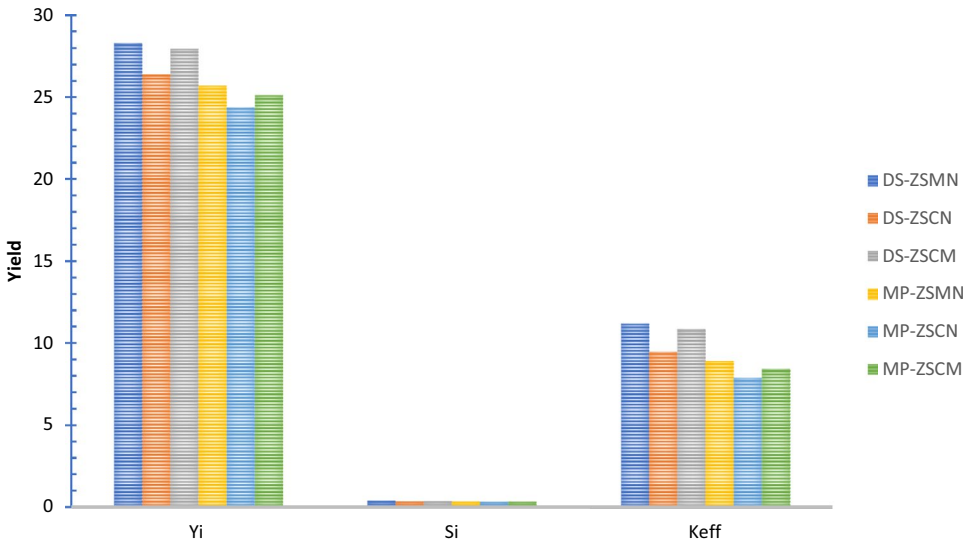

Fig. 6 Comparison of the yield, selectivity and effectiveness of the catalysts

[23]. Compared to the other biomass species, date seed and mandarin peel were found to have quite low H/C values like 1.24 and 1.29, respectively [17, 21] as can be found in Table S1 in Supplementary File. Thus, the biomass nature is also one of the parameter affecting the catalyst activity as well.

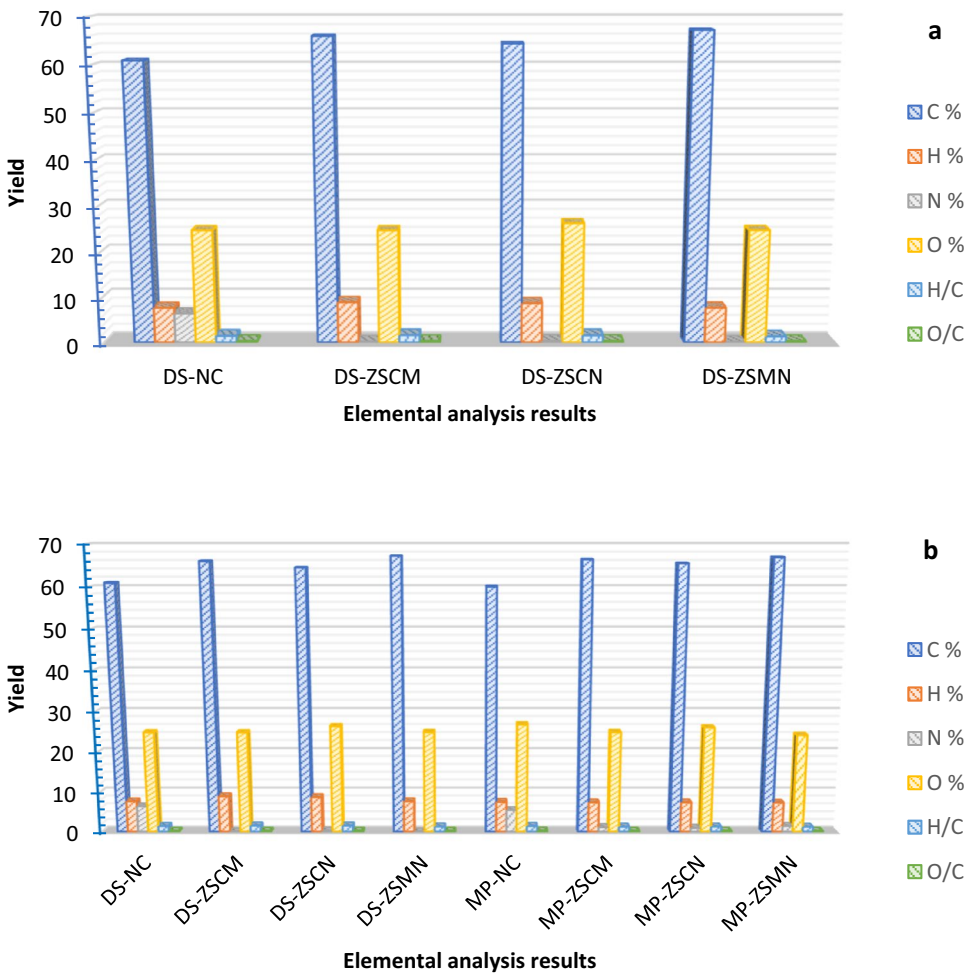

Fig. 7 Elemental analysis results of the non-catalytic and catalytic bio-oils **a** date seed and **b** mandarin peel

3.3 Characterization of Bio-oils

Elemental analysis results of the non-catalytic and catalytic bio-oils are given in Fig. 7. The results showed that the catalysts favored to decline the oxygen content and rise the carbon and hydrogen content. Comparing of H/C ratios with conventional fuels indicated that the H/C ratios of the bio-oils fall between those of heavy and light petroleum products. Indeed, the HHV of the date seed bio-oil and mandarin peel bio-oil were calculated as 27.31 MJ/kg and 26.44 MJ/kg which are remarkable but the catalysts further improved the heating value of bio-oils into a range of 29.46–30.87 MJ/kg for date seed catalytic bio-oils and 28.23–28.94 MJ/kg for mandarin peel catalytic bio-oils. This rise could be ascribed to the decline in oxygen [21].

Bio-oil achieved from pyrolysis of biomass is known to have a very complex structure. FT-IR spectrum of the bio-oils were shown in Figs. 8 and 9. The comprehensive analysis of the functional groups is approved the existence of both aromatic and acyclic groups of compounds in the bio-oil. When the spectra were compared, the results were found quite similar to each other. There are some differences between thermal and catalytic bio-oil spectra which can be expected from elemental analysis results as well. The O–H stretching vibrations between 3200 and 3600 cm^{-1} showed the presence of phenols and alcohols. This peak was quite reduced in terms of catalytic pyrolysis for both biomass existences. The occurrence of alkanes was displayed by the peak of C–H vibrations between 3000 and 2800 cm^{-1} and by 1490–1325 cm^{-1} bands related to the C–H bending. The C=O stretching vibrations with absorbance peaks between 1650 and 1775 cm^{-1} signified the presence of aldehydes, ketones, carboxylic acids and esters. Indeed, C=C presented in olefinic vibrations in aromatic region. The occurrence of O–H and C–O stretching vibrations together indicated the presence of carboxylic acids and derivatives. For especially date seed catalytic pyrolysis, this peak (almost at 1750 cm^{-1}) eliminated. The peaks between 1680 and 1575 cm^{-1} indicated the incidence of alkanes and nitrogenated compounds. The peaks between 1300 and 950 cm^{-1} was belong to primary, secondary and tertiary alcohols and phenols displaying the C–O stretching and O–H bending. For both catalytic bio-oils, this peak disappeared. The existence of polycyclic, single, and substituted aromatic groups could be approved from the absorbance peaks between 900 and 650 cm^{-1}. The intensity of this peak was increased with catalyst presence.

For mandarin peel bio-oils, almost same peaks but different in intensities observed. The peak intensity at almost 3400 cm^{-1} was more evident than date seed thermal pyrolysis which was also expected from elemental analysis. When the catalysts used, this peak intensity decreased as well as at 1000 cm^{-1} and 800 cm^{-1} that were respect to C–O stretching and O–H bending, and presence of polycyclic, single, and substituted aromatic groups, respectively. The peak at 2900 cm^{-1} which presence of alkanes was higher in intensity with catalyst usage. The C=C skeletal vibration at 422 cm^{-1}

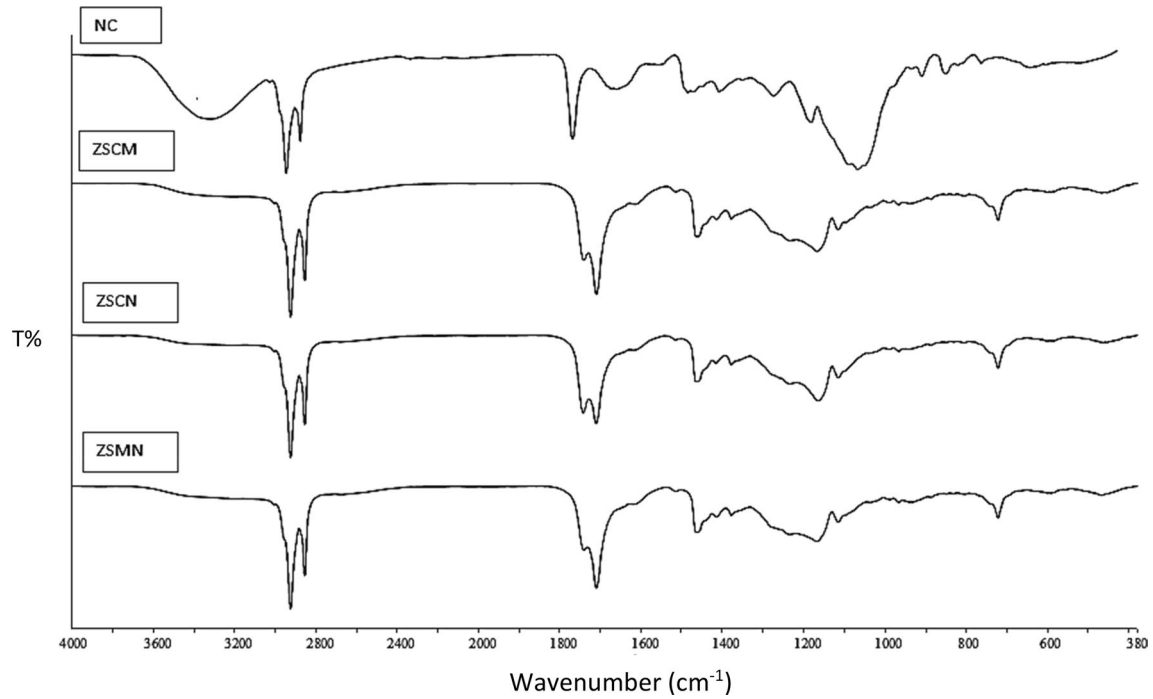

Fig. 8 FT-IR spectrum of DS thermal and catalytic bio-oils

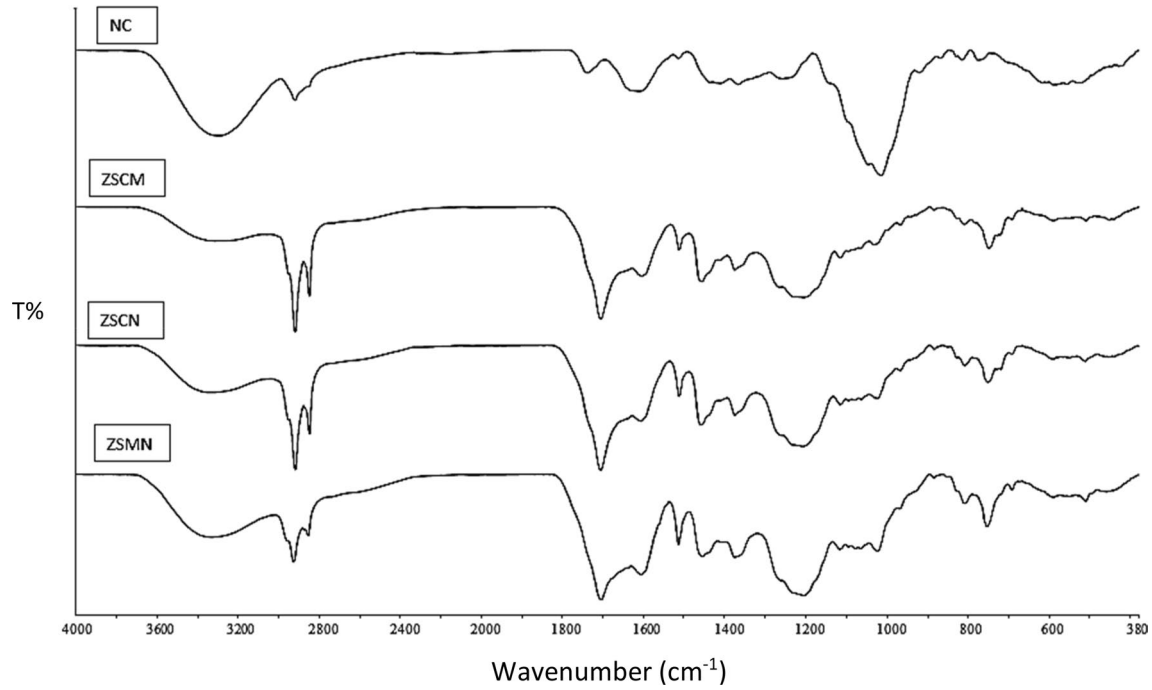

Fig. 9 FT-IR spectrum of MP thermal and catalytic bio-oils

was related to the existence of alkenes in fatty acid chains for mandarin peel bio-oils.

Although the O–H and N–H stretching vibrations at 2353 cm^{-1} was not obtained for non-catalytic DS and MP pyrolysis bio-oils, there was a slight curve indicating the existence of benzene ring compounds with hydroxyl and amine bond in catalytic runs. The C–C skeletal vibration at 975 cm^{-1} specified the presence of cyclic compounds which is quite evident for non-catalytic bio-oils.

GC–MS was used to identify the bio-oil compositions. Figure 10 shows the product distribution of the bio-oils obtained by non-catalytic and catalytic pyrolysis. As given in the literature, acids, PAHs, esters and ethers are classified as the undesired products from pyrolysis, however phenols, hydrocarbons, furans, and alcohols can be identified as desirables for fuel and valuable chemical production [21]. Compounds that cannot be detected by the GC–MS system were classified as non-detected products. The major compounds in the both biomass` bio-oils were found to be phenol, 2-methyl phenol, 4-methyl phenol, 3-ethyl phenol, methyl ester-9-octadecenoic acid, pentadecanoic acid and undecane. The bio-oils also contained significant amount of 1-dodecene, dodecane, 1-tridecene, tetradecane, heptadecane. These chemicals were faced in many bio-oils present in literature [17, 21]. The bio-oil was contained with high amount of aromatic and phenolic compounds. Phenol is recognized to be the pioneer of many compounds such as resins, plastics and adhesives [24, 25]. While degradation of biomass takes place, the interaction between hemicellulose and lignin forms phenol as a pyrolytic product. The alkanes in the bio-oil are generally related to the extractive content. It is known that benzene, phenols, cresols and many additional aromatic compounds formed from pyrolysis of lignin [25].

The bio-oil obtained from non-catalytic date seed was found higher in phenolics, hydrocarbons, esters and ketones compared the bio-oil from thermal pyrolysis of mandarin peel. Mandarin peel non-catalytic bio-oil was found to have higher alcohol content than date seed non-catalytic bio-oil. Alcohol is known as useful for making of fuel and various solvents [25]. Pentadecanoic Acid was mainly derived from the cracking of cellulose and hemicellulose [26].

Using perovskite type catalysts affected each biomass in terms of different compound yield. For instance, in case of date seed, perovskites yielded an increment in alcohols and esters. The decline in phenolics and hydrocarbons in catalytic bio-oils can be detected easily. Perovskite catalyst promoted cracking of hemicellulose and cellulose, consequently decreased the content of phenols in bio-oil. Besides, the increment of O-species was mainly related to the deoxygenation effect of perovskite catalysts. Furthermore, O-species intermediates do not provide hydrogen for the generation of phenols that possibly will cancel to proceed deoxygenation reactions during these process.

Catalytic pyrolysis with mandarin peel as a biomass showed an increasing tendency for hydrocarbons, esters, ketones and furans. Alcoholic compounds content was decreased with perovskites for mandarin peel pyrolysis as

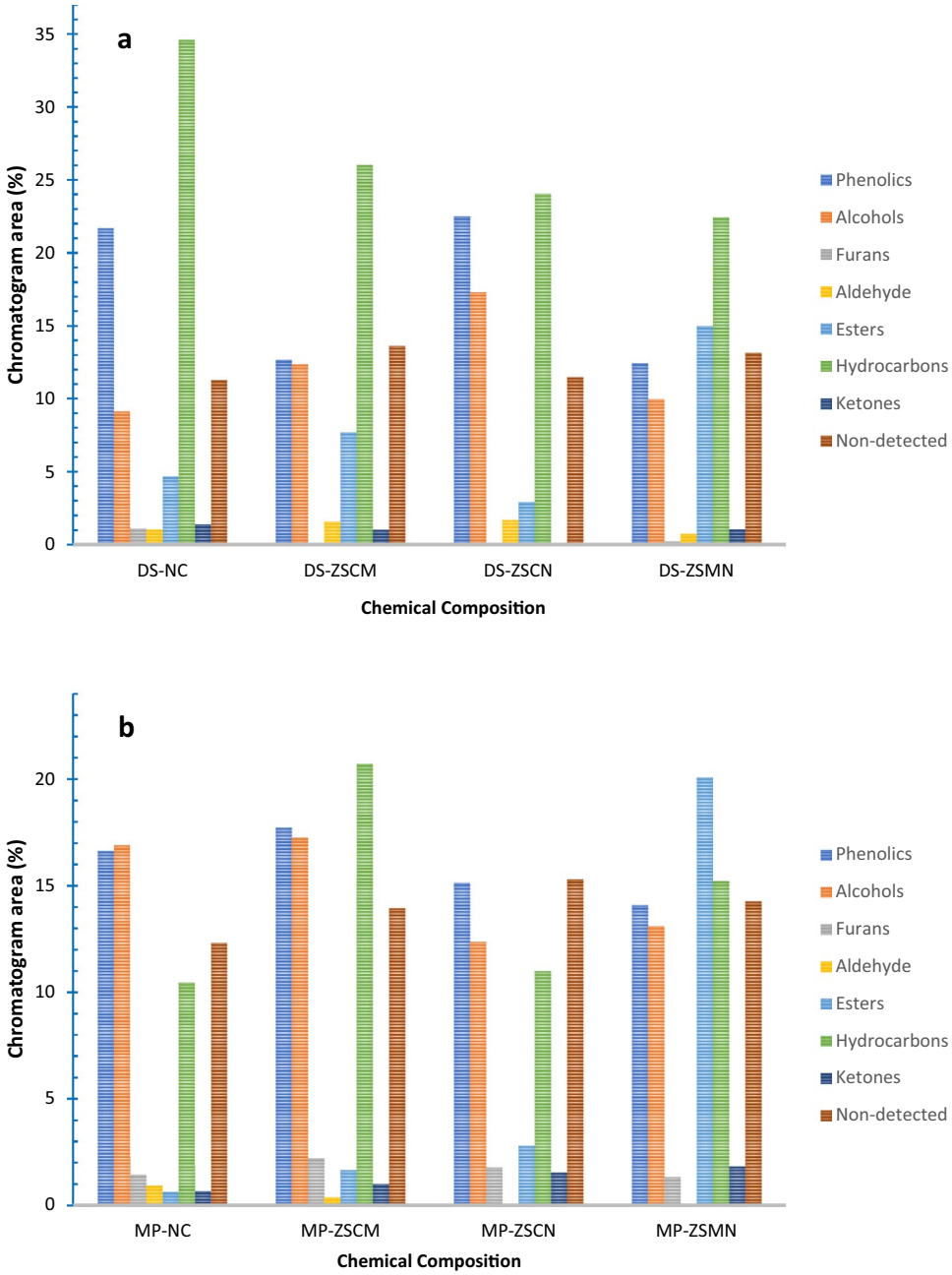

Fig. 10 GC–MS results in terms of chemical composition of non-catalytic and catalytic pyrolysis bio-oils **a** date stone, **b** mandarin peel

Table 2 ^{1}H-NMR results of bio-oils as percentage hydrogen total

Proton assignment	Chemical shift region (ppm)	DS	DS-ZSMN	MP	MP-ZSMN
CH_3 γ or further from an aromatic ring	0.5–1.0	10.23	12.75	4.38	8.51
β -CH_3, CH_2 and CH γ or further from an aromatic ring	1.0–1.5	45.00	38.36	32.89	27.05
CH_2 and CH β to an aromatic ring (napthenic)	1.5–2	8.70	6.61	10.38	11.03
CH_3. CH_2 and CH to an aromatic ring	2.0–3.0	13.25	13.03	12.86	7.82
Ring-joinmethylene (Ar-CH_2-Ar)	3.0–4.5	4.23	4.70	13.12	14.53
Phenolic (OH) or olefinic proton	4.5–6.0	12.66	16.72	7.74	11.68
Aromatic	6.0–9.0	5.93	7.83	18.62	19.39
Aldehydes (R-CHO) and/or carboxylic acids (R-COOH)	9.0–12.0	–	–	–	–

well as date seed pyrolysis. A small increment was observed for phenolics for mandarin peel.

^{1}H-NMR spectra were obtained for non-catalytic and optimum $LaMn_{0.5}Ni_{0.5}O_3$ catalyst used bio-oils and the results are given in Table 2. After evaluating at the spectra of mandarin peel liquid products, aliphaticity was obtained compared to the catalytic liquid products of date stone. In contrast, aromatics and conjugated olefins have increased considerably. It has been observed that element B added to the structure within the scope of synergistic effect reduces total aliphatic values. Aromatics, phenols, conjugated and non-conjugated olefins increased with synergistic effect catalysts. Table 2 also confirms that the liquid products of the date stone contain predominantly aliphatic compounds. The presence of phenols, unconjugated olefins after aliphatics draw attention. It has been observed that element B added to the structure within the scope of synergistic effect reduces total aliphatic values.

According to the ^{1}H-NMR results, it has been observed that all synthesized catalysts reduce total aliphatic values, increase phenols and aromatics. This is compatible with GC/MS chromatograms.

4 Conclusion

A strategy such a B′ site doping has been applied to perovskite in order to improve its effectiveness on yield as well as properties of bio-oil obtained from different biomass'. The key conclusions of this paper were drawn as follows:

- Doping of metals was found as a useful procedure to modify, and improve the properties of the catalysts. From the bio-oil yields point of view, all the catalysts used increased the bio-oil yields. ZSMN was the most effective catalyst and improved the bio-oil yields than non-catalytic ones for all biomass species.
- According to bio-oil characterization results view, perovskites favored to decline the oxygen content and rise the carbon and hydrogen content. The comprehensive analysis of the functional groups is approved the existence of both aromatic and acyclic groups of compounds in the bio-oil.
- The major compounds in the both biomass bio-oils were found to be phenol, 2-methyl phenol, 4-methyl phenol, 3-ethyl phenol, methyl ester-9-octadecenoic acid, pentadecanoic acid and undecane. Using perovskite type catalysts affected each biomass in terms of different compound yield. For instance, in case of date seed usage, the perovskites yielded increment in alcohols and esters. The decline in phenolics and hydrocarbons in catalytic bio-oils can be detected easily. Catalytic pyrolysis with mandarin peel as a biomass showed increasing tendency for hydrocarbons, esters, ketones and furans. Alcoholic compounds content was decreased with perovskites for mandarin peel pyrolysis as well as date seed pyrolysis.
- Prior to non-catalytic and catalytic pyrolysis results, date seed was found superior than mandarin peel when bio-oil yield and quality considered. Even in case of conversion, the mandarin peel more favorable.

According to the results, synergetic effect of metal species co-substitution in perovskite type catalysts for biomass pyrolysis can significantly increase the catalyst performance which affects biomass conversion and bio-oil quality directly. Utilizing co-substitution property of the perovskites is offered in biomass pyrolysis system. The synergetic effect of metal species co-substitution serves an offer to evaluate this advantage in large-scale bio-oil production processes.

Funding This research did not receive any specific Grant from funding agencies in the public, commercial, or not-for-profit sectors.

References

1. Tabakaev R, Kanipa I, Astafev A et al (2019) Thermal enrichment of different types of biomass by low-temperature pyrolysis. Fuel 245:29–38. https://doi.org/10.1016/j.fuel.2019.02.049
2. Johansson AC, Wiinikka H, Sandström L et al (2016) Characterization of pyrolysis products produced from different Nordic biomass types in a cyclone pilot plant. Fuel Process Technol 146:9–19. https://doi.org/10.1016/j.fuproc.2016.02.006
3. Oasmaa A, Solantausta Y, Arpiainen V et al (2010) Fast pyrolysis bio-oils from wood and agricultural residues. Energy Fuels 24(2):1380–1388. https://doi.org/10.1021/ef901107f
4. Uzun BB, Sarioğlu N (2009) Rapid and catalytic pyrolysis of corn stalks. Fuel Process Technol 90(5):705–716. https://doi.org/10.1016/j.fuproc.2009.01.012
5. Iliopoulou EF, Stefanidis S, Kalogiannis K et al (2014) Pilot-scale validation of Co-ZSM-5 catalyst performance in the catalytic upgrading of biomass pyrolysis vapours. Green Chem 16(2):662–674. https://doi.org/10.1039/c3gc41575a
6. Lappas AA, Kalogiannis KG, Iliopoulou EF et al (2012) Catalytic pyrolysis of biomass for transportation fuels. Wiley Interdiscip Rev Energy Environ 1(3):285–297. https://doi.org/10.1002/wene.16
7. Yaman E, Yargic AS, Ozbay N et al (2018) Catalytic upgrading of pyrolysis vapours: effect of catalyst support and metal type on phenolic content of bio-oil. J Clean Prod 185:52–61. https://doi.org/10.1016/j.jclepro.2018.03.033
8. Zhao K, Chen J, Li H et al (2019) Effects of Co-substitution on the reactivity of double perovskite oxides $LaSrFe_{2-x}Co_xO_6$ for the chemical-looping steam methane reforming. J Energy Inst 92(3):594–603. https://doi.org/10.1016/j.joei.2018.03.013
9. Zhang J, Tan D, Meng Q et al (2015) Structural modification of $LaCoO_3$ perovskite for oxidation reactions: the synergistic effect of Ca^{2+} and Mg^{2+} co-substitution on phase formation and catalytic performance. Appl Catal B 172–173:18–26. https://doi.org/10.1016/j.apcatb.2015.02.006
10. Liu J, Lu S, Wang L et al (2019) Co-site substitution by Mn supported on biomass-derived active carbon for enhancing

magnesia desulfurization. J Hazard Mater 365:531–537. https://doi.org/10.1016/j.jhazmat.2018.11.040
11. Cihlar J, Vrba R, Castkova K, Cihlar J (2017) Effect of transition metal on stability and activity of La-Ca-M-(Al)-O (M = Co, Cr, Fe and Mn) perovskite oxides during partial oxidation of methane. Int J Hydrogen Energy. 2(31):19920–19934. https://doi.org/10.1016/j.ijhydene.2017.06.075
12. de Santana SM, Neto RCR, Noronha FB et al (2018) Perovskite as catalyst precursors in the partial oxidation of methane: the effect of cobalt, nickel and pretreatment. Catal Today 299:229–241. https://doi.org/10.1016/j.cattod.2017.06.027
13. Machin NE, Karakaya C, Celepci A (2008) Catalytic combustion of methane on La-, Ce-, and Co-based mixed oxides. Energy Fuels 22(4):2166–2171. https://doi.org/10.1021/ef8000983
14. Wang J, Su Y, Wang X et al (2012) The effect of partial substitution of Co in $LaMnO_3$ synthesized by sol-gel methods for NO oxidation. Catal Commun 25:106–109. https://doi.org/10.1016/j.catcom.2012.04.001
15. Zhang C, Wang X, Wang Z et al (2016) Dielectric relaxation, electric modulus and ac conductivity of Mn-doped $YFeO_3$. Ceram Int. 42(16):19461–19465. https://doi.org/10.1016/j.ceramint.2016.09.037
16. Yarbay RZ, Figen HE, Baykara SZ (2012) Effects of cobalt and nickel substitution on physical properties of perovskite type oxides prepared by the sol-gel citrate method. Acta Phys Pol, A 121(1):44
17. Ozbay N, Yargic AS, Yarbay Sahin RZ (2016) Tailoring Cu/Al_2O_3 catalysts for the catalytic pyrolysis of tomato waste. J Energy Inst. 91(3):424–433. https://doi.org/10.1016/j.joei.2017.01.010
18. Wang C, Pan J, Li J, Yang Z (2008) Comparative studies of products produced from four different biomass samples via deoxyliquefaction. Bioresour Technol 99(8):2778–2786. https://doi.org/10.1016/j.biortech.2007.06.023
19. Karagöz S, Bhaskar T, Muto A, Sakata Y (2005) Comparative studies of oil compositions produced from sawdust, rice husk, lignin and cellulose by hydrothermal treatment. Fuel 84(7–8):875–884. https://doi.org/10.1016/j.fuel.2005.01.004
20. Maisano S, Urbani F, Mondello N, Chiodo V (2017) Catalytic pyrolysis of Mediterranean sea plant for bio-oil production. Int J Hydrogen Energy 42(46):28082–28092. https://doi.org/10.1016/j.ijhydene.2017.07.124
21. Ozbay N, Yargic AS, Yarbay Sahin RZ, Yaman E (2019) Valorization of banana peel waste via in-situ catalytic pyrolysis using Al-Modified SBA-15. Renew Energy 140:633–646. https://doi.org/10.1016/j.renene.2019.03.071
22. Özbay N, Yarbay Şahin RZ (2020) Effect of preparation method and B-side metal type on the physicochemical properties of $LaBO_3$ perovskite catalyst and its catalytic behaviour in the biomass pyrolysis. Biomass Convers Bioref. https://doi.org/10.1007/s13399-020-00925-523
23. Shafaghat H, Lee HW, Tsang YF et al (2019) In-situ and ex-situ catalytic pyrolysis/co-pyrolysis of empty fruit bunches using mesostructured aluminosilicate catalysts. Chem Eng J 366:330–338. https://doi.org/10.1016/j.cej.2019.02.055
24. Mishra RK, Mohanty K (2019) Pyrolysis of three waste biomass: effect of biomass bed thickness and distance between successive beds on pyrolytic products yield and properties. Renew Energy 141:549–558. https://doi.org/10.1016/j.renene.2019.04.044
25. Chatterjee G, Shadangi KP, Mohanty K (2018) Fuel properties and composition study of Cassia siamea seed crude pyrolytic oil and char. Fuel 234:609–615. https://doi.org/10.1016/j.fuel.2018.07.066
26. Chen W, Fang Y, Li K et al (2020) Bamboo wastes catalytic pyrolysis with N-doped biochar catalyst for phenols products. Appl Energy 260:114242. https://doi.org/10.1016/j.apenergy.2019.114242

Affiliations

Rahmiye Zerrin Yarbay Şahin[1,2] · Nurgül Özbay[1]

✉ Rahmiye Zerrin Yarbay Şahin
zerrin.yarbay@bilecik.edu.tr

[1] Chemical Engineering Department, Faculty of Engineering, Bilecik Şeyh Edebali University, Gulumbe Campus, 11230 Bilecik, Turkey

[2] Energy Technologies Application and Research Centre, Bilecik Şeyh Edebali University, 11230 Bilecik, Turkey